

Gravity Probe B GPS Orbit Determination with Verification by Satellite Laser Ranging

G. Hanuschak¹, H. Small¹, D. DeBra¹, K. Galal², A. Ndili¹, P. Shestopole¹.

¹Gravity Probe B, Hansen Experimental Physics Laboratory, Stanford University, Stanford CA, 94044

²NASA Ames Research Center, Moffett Field, CA, 94035

BIOGRAPHY

Gregor Z. Hanuschak is a graduate student of Aeronautics and Astronautics at Stanford University and lead orbit determination analyst at Gravity Probe B.

Hunt Small is an orbit specialist consulting on GP-B orbit operations.

Dan DeBra is professor emeritus of Aeronautics and Astronautics at Stanford University and Co-PI of the Gravity Probe B mission.

Ken Galal is a Flight Dynamics Engineer at NASA's Ames Research Center and manager of GP-B orbit operations.

Awele Ndili is a GPS researcher at the Gravity Probe B program at Stanford University and CEO of MShift, Inc.

Paul Shestopole is the GPS responsible engineer for the Gravity Probe B program at Stanford University.

ABSTRACT

The Gravity Probe B (GP-B) satellite has recently completed its science mission. The payload is equipped with two redundant TANS Vector III GPS receivers, used to reconcile vehicle time with Coordinated Universal Time (UTC) and to provide coarse satellite position data. GPS position accuracy easily outperforms mission requirements of 100 m RMS per axis for onboard solutions. The GP-B precision orbit is determined in ground processing of 30-hour and 18-hour GPS data segments using MicroCosm software. Overlaps of consecutive 18-hour ephemeris segments are found to have maximum position errors whose RMS is 2.5 meters, and maximum velocity errors whose RMS is 2.2 mm/sec. Satellite Laser Ranging (SLR) measurements provide independent verification of the GPS-derived GP-B orbit. This paper begins with a brief background of the GP-B mission including a description of the GPS equipment and

orbit determination operations. GP-B ephemeris errors estimated using ephemeris overlap comparisons and SLR residual computations are detailed. We conclude with a brief description of in-progress investigations that are anticipated to improve results.

INTRODUCTION

The Gravity Probe B (GP-B) spacecraft (depicted in Figure 1) is designed to test Einstein's General Theory of Relativity. This is accomplished by monitoring the drift rate of spinning mechanical gyroscopes in an inertial frame isolated from Newtonian torques. The four gyros are mounted inside the GP-B spacecraft, which moves in a near-polar, near-circular orbit at close to 640 km altitude. The vehicle rolls at 0.77 rpm about its telescope axis, pointed towards a guide star, IM Pegasi (a member of the constellation Pegasus). Hence, the spacecraft's attitude is unique: a low earth orbit, with a stabilized inertia as it points towards a sole guide star, rotating continually. Please see reference [1] for further details regarding the GP-B mission.

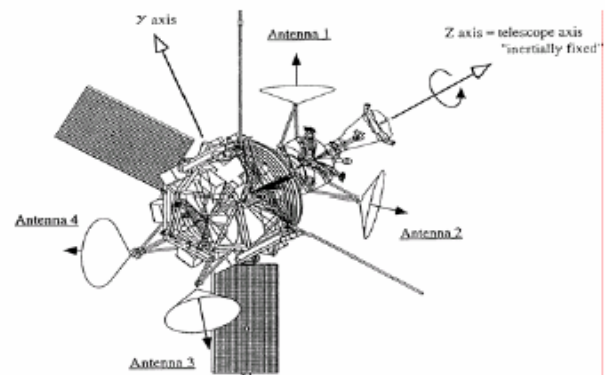


Figure 1: GP-B Satellite with GPS equipment

The GPS equipment on GP-B is divided into two fully redundant sets. Each set is composed of a Trimble TANS Vector III GPS receiver and four matching Trimble antennas modified for space use by Stanford University.

The Trimble TANS Vector III is a six channel L1 receiver which calculates position, velocity, and time (PVT) every 1.7 seconds. The receivers are mounted on the spacecraft superstructure (Figure 1). Each receiver has inputs for four antennas (two mounted fore and two aft) placed so as to maximize antenna baseline and optimize sky view. The forward antenna's fields of view are obstructed slightly by the telescope sun shade, but otherwise the antennas enjoy a full view of the sky. Please see reference [2] for a complete description of the GP-B GPS equipment.

GPS telemetry is the primary source of position and velocity information. Satellite Laser Ranging solutions are used to verify GPS orbit measurements during the mission. Two hours after launch, the GPS receiver was turned on. Real time position and velocity telemetry provides relatively coarse orbit solutions. Post processed telemetry provides more precise orbit solutions. Accurate orbit solutions are needed to determine the extent of orbit trim required during the initialization phase of the mission, and for precise vehicle position and velocity knowledge during the science and calibration phases of the mission.

ORBIT DETERMINATION

GP-B operations require knowledge of the satellite ephemeris. Moderately accurate position and velocity data are needed for routine mission operations planning and scheduling. More stringent requirements specify 25 m and 7.5 cm/sec RMS position and velocity accuracy, respectively, to permit accurate relativistic drift scaling, and to calculate aberration signatures used for science signal calibration.

For those purposes, GP-B ephemeris segments are generated every day using independent batch fits to 30-hour spans of GPS position data centered on Greenwich noon. The resulting 6-hour overlaps before and after each segment are used for consistency comparisons.

In order to achieve the required orbit accuracy during certain spans of the science mission it was found necessary to supplement the usual daily batch fits with supplemental fits. Those used 18 hour data spans centered on 0600 and 1800 hours and two additional empirical solve-for parameters. Those and other upgrades are discussed below after showing the results from the routine daily data processing.

Satellite Laser Ranging measurements have been available since late July 2004. Because laser contact data are often sparse (occasionally no passes or one pass per day for several contiguous days) and often ill-conditioned, it is frequently not possible to generate comparable independent daily ephemeris segments from laser data

alone. Nevertheless, individual SLR measurements are used to compute range residuals from the GPS-based ephemeris. This process provides independent verification of the GPS ephemeris.

GPS Data

GPS solutions, using GPS almanacs, are telemetered to the ground at 10-second intervals. Data are filtered for duplicate points and points which fall outside a reasonable radius and velocity window. The result is a dataset that typically contains 82% of available points in each 30-hour segment. As noted elsewhere in these proceedings, a switch from the A-side to the B-side receiver on March 7th 2005 caused a reduction in available points to 74%.

Either data set is more than adequate: tests showed that a GP-B ephemeris that meets requirements could be pieced together from fits to 6-hour hour segments. Both position and velocity vectors were available at each time point, but the fractional errors in velocity data were substantially worse than those in position data, ($\Delta V/V \approx 5 \Delta R/R$), so only position data were used.

SLR Data

SLR data consist of round-trip range measurements to the GP-B spacecraft from an international network of laser ranging ground stations. Individual SLR measurements are more accurate than a GPS measurement, but orbit determination, which estimates the path between those points, depends very much on the particulars of the data set available.

Orbit determination (OD) accuracy from laser ranging measurements is dependent on the number of passes and the spatial distribution of those passes over the solution interval. An attempt is made to obtain as many observations as possible, but it is impossible to control factors such as weather. Approximately 50% of the time, weather conditions such as cloud cover do not allow for laser ranging. In addition, due to GP-B's inertial pointing attitude and the placement of its retro-reflectors (on the

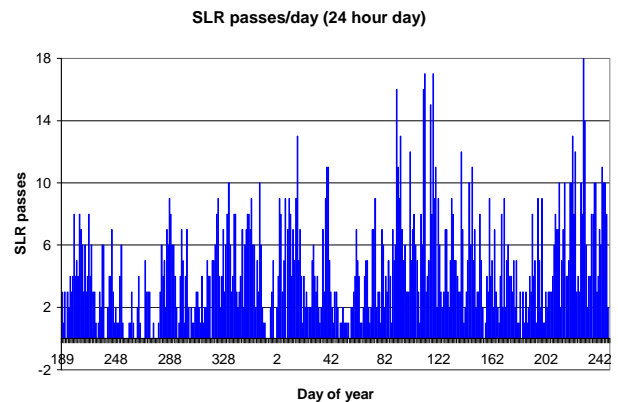


Figure 2: SLR passes per day

aft end of the spacecraft), as well as mask angle limitations of the laser range stations, laser measurements can only be taken to the portion of the orbit closest to the guide star and mostly only over the Northern Hemisphere.

Figure 2 shows a history of GP-B SLR passes to date. SLR tracking was initiated in late-July of 2004, and passes have varied from 0 to 18 passes per day. An average of 5 SLR passes are collected per day. That was not sufficient to make daily OD fits with accuracy comparable to the GPS fits, but it was very useful in supplying accurate range values used to validate the GP-B ephemeris obtained from GPS data.

FORCE MODELING

The commercial software package MicroCosm is used to fit an ephemeris to the data. The 35 x 35 gravity model JGM3 is used for these fits, along with luni-solar and earth-tide effects, a constant (shadowed) radiation pressure model and a Jacchia '71 atmospheric density model, both with adjustable scale factors.

The geo-potential model used was a compromise between accuracy and computational efficiency. The geo-potential error contribution to the GP-B ephemeris was estimated by using the 35x35 jgm3 model to fit a 30-hour ephemeris generated from the much newer 99x99 GGM02 geo-potential model. The RMS position residual of that fit was less than 2 meters – much less than the GPS data noise – so the lower degree and order geo-potential is considered adequate for GP-B OD. (The 50x50 GGM02 geo-potential was used during the 18-hour fits discussed below. A similar evaluation of the 50x50 model when it was used to fit the ephemeris generated with the 99x99 GGM02 geo-potential showed RMS position errors less than 0.3 meter.)

The GP-B spacecraft uses helium boil-off from the Dewar to control attitude and roll rate by metering the gas through eight pairs of micro-thrusters. Any excess gas is nominally vented through opposing thrusters in order to avoid imparting unwanted torques or translational forces on the spacecraft.

Empirical parameters were included as solve-for states in the OD process in order to model GP-B axial thrusting effects. There are two types of thrusting observed. Each has been observed to contribute accelerations up to 5×10^{-7} m/sec². Each is modeled as being along the roll axis, directed always toward or away from the guide star. Because the spacecraft rolls, continuous body-fixed accelerations of order 10^{-7} m/sec² directed perpendicular to the roll axis should average out.

One type of thrusting is due to imperfectly calibrated helium outgassing. That effect is essentially constant

during any one day, but it tends to grow slowly with time. Since the initial calibration period, accelerations due to outgassing have been maintained to less than 1.5×10^{-7} m/sec² by using re-calibration commands every few months. If that acceleration is modeled with geocentric polar coordinates (G_O , U_{IN}) in the GP-B orbit plane, with U_{IN} measured from the ascending node (so $U_{IN} \approx 163^\circ$), and if A and B are the eccentricity components ($A \equiv e \cos \omega$ and $B \equiv e \sin \omega$) then from Lagrange's Variation of Parameters equations, the secular effects of that constant acceleration are found to be

$$dA/dt = 1.5 (G_O / V) \sin U_{IN} \quad (1)$$

$$dB/dt = -1.5 (G_O / V) \cos U_{IN}$$

where V is the orbital velocity. Equations (1) show that that effect perturbs the orbit by up to 20 m/day by changing the orbital eccentricity vector in the orbit plane perpendicular to the guide star direction. The effect is analogous to that of radiation pressure.

The other type of thrusting only appeared after starting 'drag free' science mode on day 242 (August 29th) of 2004. The 'drag free' control system uses helium thrusters to cancel external forces (e.g., air drag and radiation pressure) to keep the gyroscope centered in its cavity [3]. However, there are also internal forces acting locally between the spacecraft and the gyroscope. These forces have required significant additional thrusting to keep the gyroscope centered. The corresponding perturbing acceleration is observed to be nearly sinusoidal and oscillating at the reference gyroscope's polhode period. The polhode is a slow variation in the orientation of a gyroscope spinning torque free due to moment of inertia differences – see reference [4] for a complete treatment of polhoding. If this acceleration is modeled with the polar coordinates ($G_C \cos \gamma$, U_{IN}) as above, then the long-period rate of change of the GP-B orbit's semi-major axis, a, and its corresponding mean in-track perturbation, $a\delta(M+\omega)$, due to that acceleration is

$$da/dt = a (G_C / V) \sin (U_{IN} - u + \gamma) \quad (2)$$

$$a\delta(M+\omega) = a G_C (1.5 + Q/n) Q^{-2} \sin (U_{IN} - u + \gamma)$$

where V, u and n are the satellite's velocity, argument of latitude and mean motion, and $Q \equiv n - (d\gamma/dt)$.

From Equations (2), it is seen that the key perturbation parameter is the difference between the orbital period and the polhode period of the gyroscope being followed. That was gyro 3 from day 242, 2004 to day 268, then gyro 1 for about 3 weeks, then back to gyro 3. The corresponding thrusting periods and acceleration levels (computed intermittently by comparing multi-day histories of in-track satellite position with Equations (2))

are shown in Figures 3 and 4. The polhode periods of Gyros 1 and 3, computed independently from on-board measurements, are shown as solid lines in Figure 3 for comparison.

The orbital period of GP-B is 97.65 minutes, so it is seen in Figure 3 that the oscillating thrusting matched the orbital period, and Q went through zero, on day 263. Before that time the semi-major axis and in-track motion oscillated with increasing amplitudes, and after that time it oscillated with decreasing amplitudes. This is illustrated in Figure 5 which shows GP-B's in-track position relative to the position of a neighboring orbit with no thrusting over the weeks approaching that resonant condition. During the days when Q was nearly zero the semi-major axis changed at a nearly constant rate, decreasing by 130 meters before starting to oscillate again. A few days later GP-B began following Gyro 1 and the driving polhode period decreased abruptly. Then Q increased by about a factor of 4 and the in-track amplitude decreased accordingly.

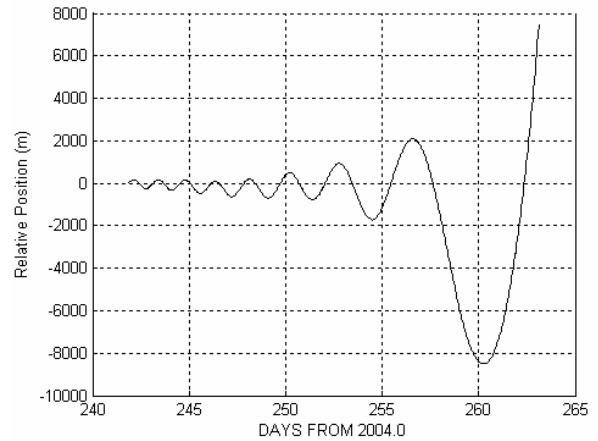


Figure 5: The in-track position of GP-B relative to a non-thrusting neighboring satellite (meters)

Ideally that axial thrusting (constant and sinusoid) would be included in the force model of the orbit determination program, using scale factors that would be fit as part of the solved-for state. The MicroCosm software does not allow for inertially fixed thrusting, but it does have the option to model unspecified in-track accelerations (G_{IT}) as a quadratic plus a sinusoid that oscillates at orbital period. That is

$$G_{IT} = a_0 + a_1 \cdot \Delta t + a_2 \cdot (\Delta t)^2 + C_A \cos u + S_A \sin u \quad (3)$$

in which u is the satellite's argument of latitude and Δt is time measured from a fixed epoch. Those accelerations cause the long period and secular changes in orbit elements

$$da/dt = (a/V) \cdot [a_0 + a_1 \cdot \Delta t + a_2 \cdot (\Delta t)^2]$$

$$dA/dt = C_A / V \quad (4)$$

$$dB/dt = S_A / V$$

$$a\delta(M+\omega) = -(3/2) [a_0 \cdot (\Delta t)^2/2 + a_1 \cdot (\Delta t)^3/6 + a_2 \cdot (\Delta t)^4/12]$$

so the 5 coefficients a_0 , a_1 , a_2 , C_A and S_A can be fit during GP-B orbit determination processing to approximate the effects on the orbit shown in equations (1) and (2).

NOMINAL ORBIT FITTING OPERATIONS

In the nominal daily GP-B ephemeris fits, the OD group solved for 9 parameters using 30-hours of GPS data centered on noon. Those parameters were the 6 state variables (position and velocity), a drag coefficient and the periodic in-track coefficients, C_A and S_A .

Throughout that period the C_A and S_A solutions served to model the observed rates of change of A and B so their solved-for values were very near to $1.5 G_O \sin U_{IN}$ and

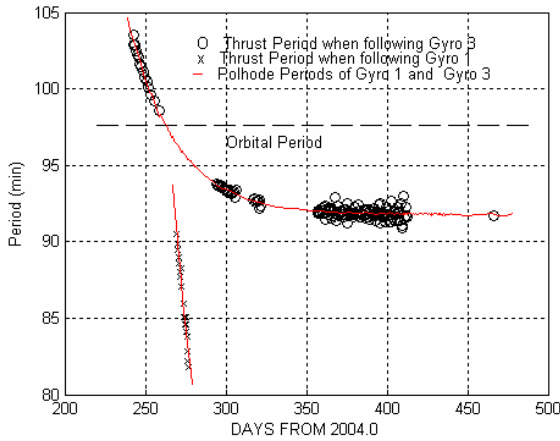


Figure 3: The Axial Thrust Period (min)

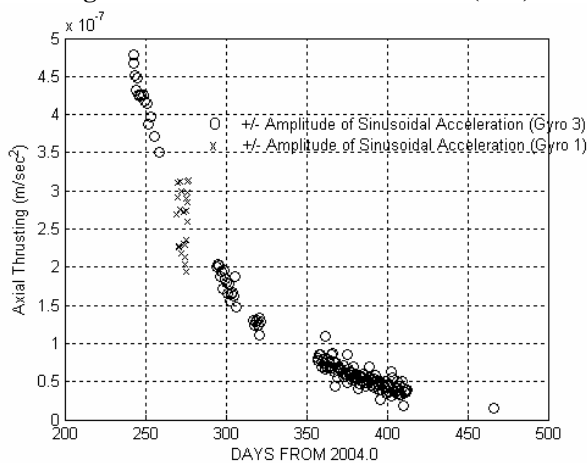


Figure 4: The Axial Thrust Amplitude (m/sec²)

$$-1.5 G_0 \cos U_{IN}$$

During initial orbit operations, before the start of the drag free mission on day 242, 2004, the drag coefficient solutions served to adjust the Jacchia '71 density model to the current density level so that the decay rate of the semi-major axis would be properly represented. After the start of drag free operations, the drag coefficient parameter still modeled changes in the semi-major axis, but not changes due to drag. During that drag free portion of the mission the daily solutions for the initial in-track position, initial angular rate and that decay rate parameter, taken together, served to model the in-track oscillations due to thrusting with 30-hour segments of best-fit quadratic arcs.

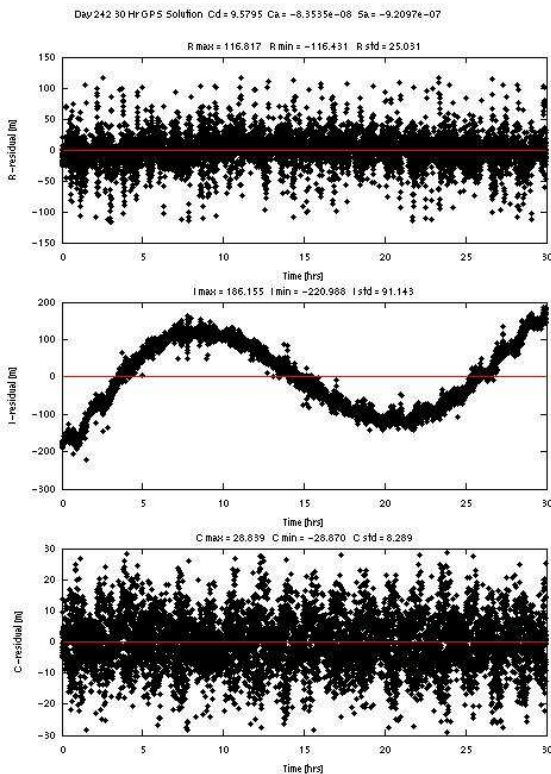


Figure 6: Typical residual plot from daily MicroCosm solution at start of drag-free operations

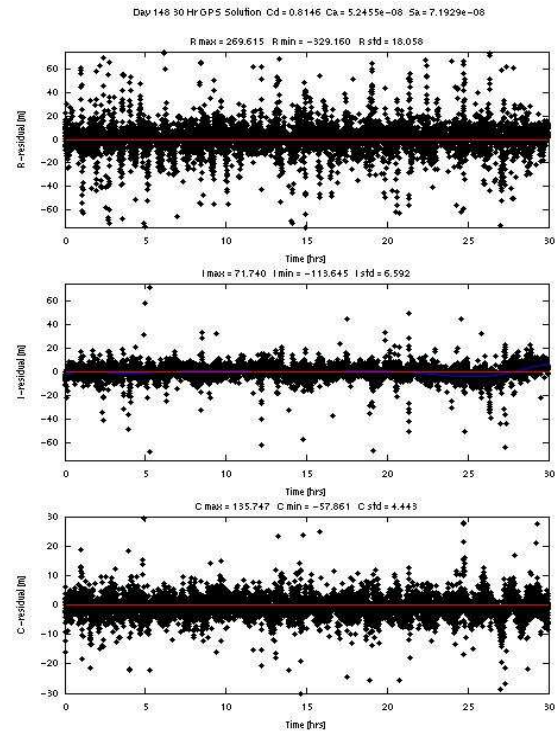


Figure 7: Typical residual plot from daily MicroCosm solution toward the end of drag-free operations

Daily plots of radial, in-track and cross-track residuals are generated to assess how well the ephemeris fits the data. Examples are shown in Figures 6 and 7. Figure 6 shows residuals for day 242, 2004, at the beginning of drag-free operations when the in-track residuals were very large, and Figure 7 shows those residuals for day 148, 2005, near the end of the mission when all residuals were small.

The details of the error magnitude variations from day to day during the mission are illustrated in Figures 8 and 9. These plots show the maximum radial, in-track and cross track position errors during the overlaps between one day's fit and the next. The cross track overlap history appears to be time independent but the radial errors and in-track errors clearly show their dependence on the histories (in Figures 3 and 4) of the sinusoidal thrusting amplitude and the corresponding difference between the thrusting period and the orbit period. The occasional error spikes in Figures 8 and 9 indicate days on which there are gaps in the GPS data or switches in and out of drag-free operations.

IMPROVED ORBIT FITTING

Recently, much of the GPS data set was reprocessed to improve the GP-B ephemeris during those times when the axial thrust accelerations were large. In the reprocessing, each daily data set was subdivided into two 18-hour sets centered on 0600 and 1800, such that there were six hour overlaps at the beginning and at the middle of each day.

These new fits used the 50x50 GGM02 geo-potential model along with luni-solar and earth tide effects. The three in-track polynomial coefficients described in Equation 3 were included as solve-for parameters, along with C_A , S_A and the orbit state vector.

Figures 10 and 11 show the new maximum position and velocity overlap errors for those time spans when GP-B was following Gyro 3 from day 242, 2004 to mid-January 2005. (In this case the plots are not subdivided into radial, in-track and cross track components. Instead, the maximum difference in all three components is plotted.) Those OD fits are evidently a great improvement over the errors at corresponding times in Figures 8 and 9, and well within GP-B requirements. The RMS values of those maximum position and velocity errors are 2.5 meters and 2.2 mm/sec respectively.

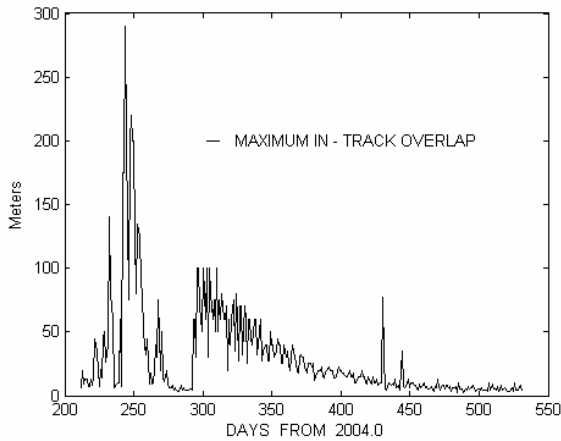


Figure 8: Maximum in-track overlap errors from nominal 30-hour OD fits (meters)

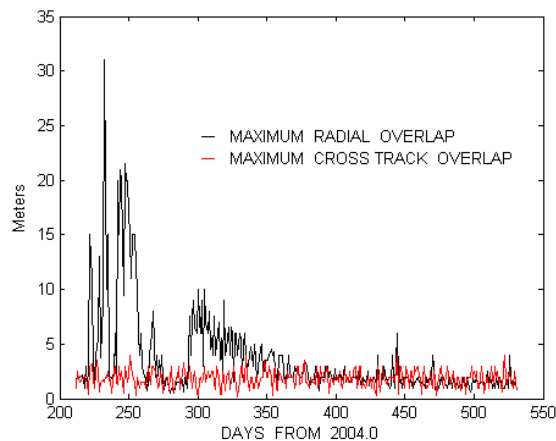


Figure 9: Maximum radial and cross-track overlap errors from nominal 30-hour OD fits (meters)

The nominal in-track fits do not satisfy the 25 m RMS orbit position requirements at all times. Since it is clear from the daily residual curves (such as Figure 6) where the GP-B satellite actually is with respect to the OD result at any time, an effort was launched to improve orbit fitting.

In addition to nominal 30-hour fits made each day, daily in-track residuals were fit to an 8th order polynomial to obtain a correction (δS) for the in-track position error and for the corresponding radial velocity error: $-n(\delta S)$. Analysis showed that these corrections could reduce overlap errors between successive corrected nominal fits, such that in-track overlap errors were rarely over 10 meters. Nevertheless, the corrected ephemeris still has the radial errors shown in Figure 9, and while those worst-case errors still have RMS values less than 25 m, there is clearly room for improvement.

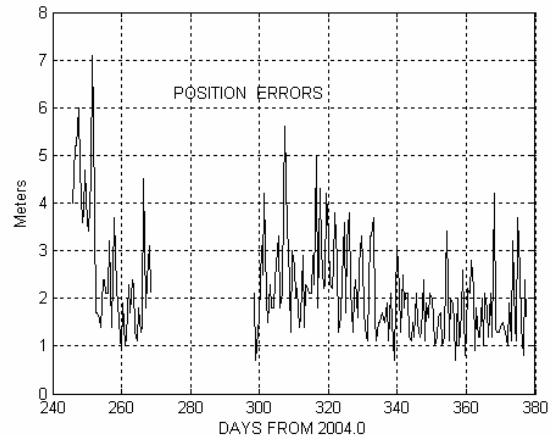


Figure 10: Maximum position overlap errors in 18-hour OD fits (meters)

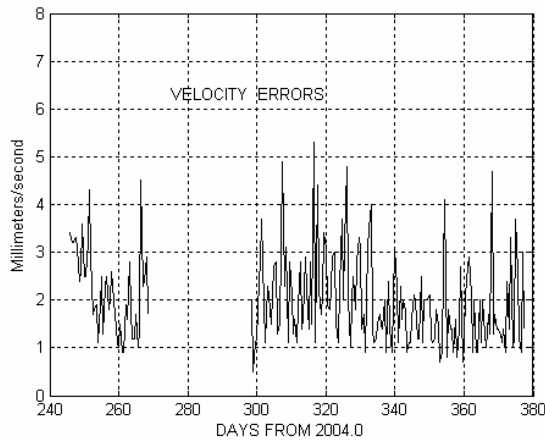


Figure 11: Maximum velocity overlap errors in 18-hour OD fits (mm / sec)

SLR COMPARISONS

An independent verification of the new 18-hour ephemeris segments was achieved using SLR. Using the GPS-derived GP-B ephemeris, SLR station-to-GP-B ranges were computed and compared to actual laser range measurements. That comparison was made by simultaneously fitting both GPS and SLR data during the OD fits, but weighting the SLR data to zero. Hence, SLR measurements had no effect on the ephemeris result but MicroCosm still produces SLR residuals.

The SLR residuals are plotted in Figure 12. Their RMS value is 2.1 meters. (Two SLR measurements that had residuals of 31 and 169 meters were omitted, but otherwise these data are unfiltered.) A correction for the known offset between the laser reflector and the center of mass of the spacecraft (1.75 meters) was not made.

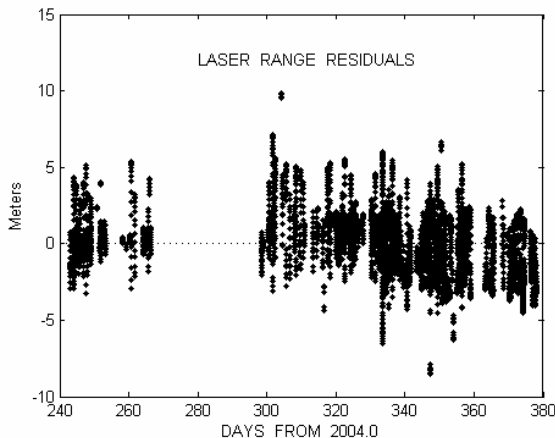


Figure 12: Comparison between GP-B 18-hour GPS ephemeris segments and SLR measurements (meters)

CONCLUSIONS

Although it had been anticipated that the ‘drag-free’ mission phase of the GP-B orbit would be free of the uncertainties of drag, radiation pressure and other non-gravitational effects, in fact unexpected internal forces acting on the gyroscopes required the introduction of compensating thrusting accelerations that were much larger than any non-gravitational force. Nevertheless, the abundance of GPS data and introduction of empirical solve-for parameters allowed the mission orbit to be fit to an accuracy well within requirements.

Nevertheless, considerable improvement can be made. The daily residual plots show that the GPS measurements have noise in the 10 to 15 meter range, due in large degree to the use of the real time GPS almanac values of GPS position and clock bias. Those errors can be greatly reduced by using the post-flight IGS almanac values, and by correcting for the difference between the GPS receivers’ positions in the GP-B spacecraft and the spacecraft center of mass. An effort to achieve 5-cm orbit accuracy is in progress.

In addition, force modeling may be significantly improved by obtaining a deeper understanding and better analytical description of the physics of the ‘polhode motions’ of the gyroscopes and the resulting compensating thrust accelerations. MicroCosm software modifications that allow direct inertial acceleration modeling, without resorting to polynomial approximations, would also enhance modeling accuracy.

ACKNOWLEDGMENTS

The authors have the deepest gratitude to those who laid the ground work for GPS on GP-B, particularly Bradford Parkinson, Penina Axelrad, Clark Cohen, George King, Glenn Lightsey, Ming Lou, Ken Schrock, Doug Simpson, Hiro Uematsu, Denys Vanrenen, Lisa Ward, David Yale, and Riaz Zaidi. Thanks to Michael Salomon and David Santiago for their investigation of the polhode motions. Thanks also to Mike Pearlman of Harvard, Carey Noll, Julie Horvath, Roberto Rodriguez, and Scott Wetzell of Goddard, and others with the International Laser Ranging Service for their support of GP-B. Special thanks to Tom Van Martin, founder of Van Martin Systems, Inc. for his extensive support of MicroCosm® software.

This work was accomplished under NASA funding, Contract No. NAS8-39225. Trimble Navigation Ltd is gratefully acknowledged for their support. The authors would also like to thank Lockheed Martin Missiles and Space for their technical support and facilities.

REFERENCES

1. S. Buchman, et al, "The Gravity Probe B Relativity Mission," *Adv. Space Res.* 25(6), p. 1177, 2000.
2. P. Shestopole, J. Li, A. Ndili and K. Schrock, "Gravity Probe B GPS Receivers." Proceedings of the Institute of Navigation's GNSS 2004 meeting.
3. Staff of the Space Department at Johns Hopkins University Applied Physics Laboratory and the staff of the Guidance and Control Laboratory at Stanford University, "A Satellite Freed of all but Gravitational Forces: "Triad I'," AIAA-1974-215, American Institute of Aeronautics and Astronautics, Aerospace Sciences Meeting, 12th, Washington, D.C., Jan. 30-Feb. 1, 1974.
4. Goldstein, H. *Classical Mechanics*, 2nd edition, Addison Wesley, 1980, p. 207.